SAND2007-6550C

2007 Fall Meeting of the Western States Section of the Combustion Institute
Sandia National Laboratories, Livermore, CA
October 16 & 17, 2007.

Soot formation and radiation in a laminar jet flame of prevaporized JP-8 surrogate burning in air

C. R. Shaddix and T. C. Williams

Combustion Research Facility, Sandia National Laboratories, Livermore, California 94550, USA

To provide experimental data for development and validation of models of soot formation and radiation for practical transportation fuels, a laminar coannular jet flame of prevaporized JP-8 surrogate burning in air was established and compared to ethylene and methane flames burning under nominally identical conditions. Both steady and pulsed flames were investigated, using planar laser-induced fluorescence (LIF) of OH and PAH distributions, planar laser-induced incandescence (LII) for soot concentrations, local measurements of total thermal radiation, planar measurements of graybody emission, planar 2-color pyrometry of soot field temperatures, and measurements of the soot dimensionless extinction coefficient.

1. Introduction

Laminar diffusion flames of simple hydrocarbons burning in air or in oxygen/nitrogen mixtures have frequently been studied to improve the understanding of soot formation and radiation. For application to fire phenomena, these studies have usually employed jet diffusion flames, where long flame residence times allow strong flame-radiation interactions to occur and flame dynamics may be easily studied with modulation of the fuel or air stream near the natural flame flicker frequency [1-8].

Most detailed analyses of flame chemistry and soot formation in these flames have focused on the use of light- to moderate-sooting fuels, such as methane, ethane, and ethylene, to facilitate the use of extractive probes and to moderate the extent of laser beam absorption and signal trapping in optical and laser-based measurements [3,6,7,9-12]. However, soot formation in non-premixed flames is known to be highly dependent on fuel structure [14], so for applications involving transportation fuels there has been a growing interest in applying modern diagnostic tools to flames fueled by heavier hydrocarbon fuels and fuel mixtures that resemble practical fuels. To establish reproducible and comparable fuel compositions for experiments and to facilitate detailed kinetic modeling, there has been a concerted effort to identify suitable fuel surrogates for transportation fuels composed of a small number of neat hydrocarbons [15-20].

Cooke et al. [21] and Moss and Aksit [20] have recently investigated laminar diffusion flames fueled by surrogates for aviation kerosene. Cooke et al. measured the temperature profiles and extinction limits of a non-sooting counterflow diffusion flame fueled by highly nitrogen-diluted surrogate burning in nitrogen-diluted oxygen. Moss and Aksit measured soot concentrations, gas temperature, and mixture fraction in a laminar jet diffusion flame fueled by nitrogen-diluted kerosene burning in air. The mixture fraction was deduced from a fuel tracer technique based on argon addition to the fuel vapor and was limited to near-centerline locations. Here, we report

new measurements of hydroxyl radical (OH·) distributions, the soot concentration field, local radiant emission, and the near-infrared soot emission field from laminar jet diffusion flames composed of methane, ethylene, and nitrogen-diluted JP-8 surrogate burning in air. The focus of the paper is on the results for the JP-8 surrogate flame, and selected results from the methane and ethylene flames are given for comparison purposes. The dimensionless extinction coefficient of the soot within these flames has been previously reported [22].

2. Burner

Steady, laminar overventilated coannular non-premixed jet flames were established on two burner systems designed for the study of steady and pulsed flames. One burner was designed for use of gaseous fuels and the other for the use of prevaporized liquid fuels. The burners had identical fuel tube and air coflow geometries so that direct comparisons could be made between the flames (see Figures 1 and 2). Both burners were constructed with brass fuel tubes, with an outer fuel tube diameter of 12.7 mm (½-inch) to match several previous studies on soot formation [9,11,12,23]. In contrast to previous coannular flame studies, a square burner face (129 x 129 mm) and chimney enclosure was designed so that large, flat windows could be easily installed in the chimney walls for ease of performing planar laser/optical measurements.

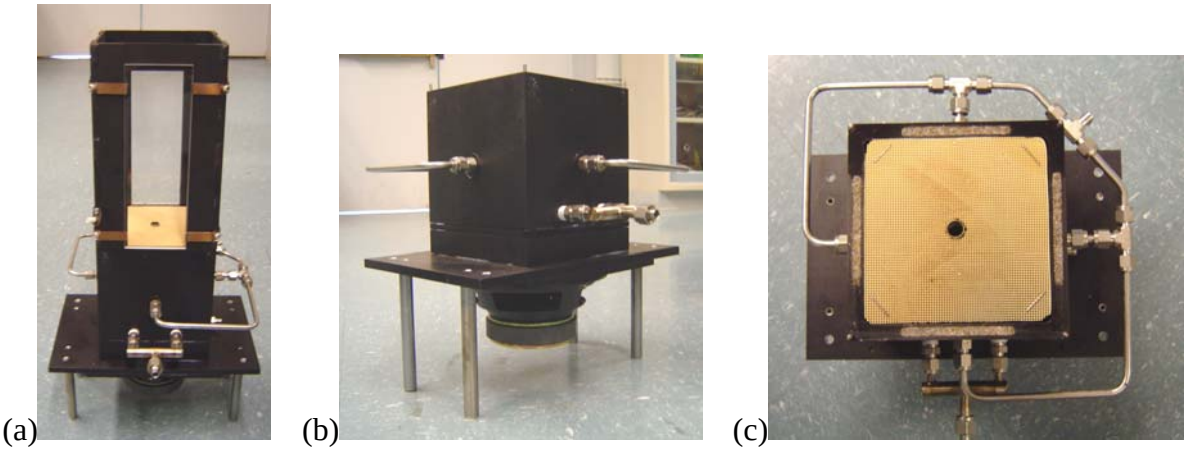

Figure 1: Photographs of coannular gas fuel burner (a) with chimney attached, showing optical access windows, (b) side profile, showing loudspeaker attached to the burner base, and (c) overhead view of the burner face, with ceramic honeycomb and central fuel tube.

Air, fuel, and nitrogen flows to the burner were metered using calibrated mass flow controllers. The fuel flowrate in the ethylene flame was chosen to match the 88 mm visible flame height of the “non-smoking” flame extensively investigated in previous studies [e.g. 9,12]. The methane flowrate was chosen to yield a similar visible flame height (84 mm). For the liquid-fueled coannular burner, a JP-8 surrogate mixture was gravity fed into a ceramic, capillary force vaporization system, which jetted vaporized fuel directly into the base of the electrically heated (350-380°C) fuel tube. The JP-8 surrogate mixture chosen was the six-component “Hex-12” surrogate developed at the University of Utah [18]. This surrogate has been shown to closely approximate the distillation curve, energy content, and smoke point (a measure of sooting

tendency) of commercial aviation kerosene and to also yield nearly identical burning rate and radiant heat flux as aviation kerosene in 30 cm diameter pool fires [18].

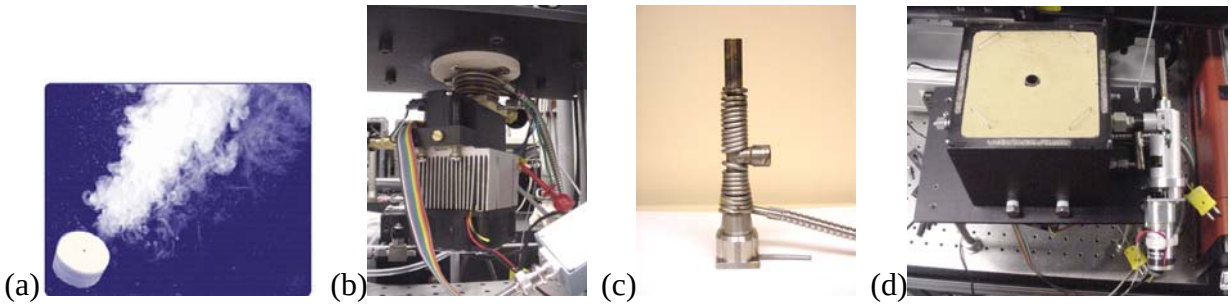

Figure 2: Photographs of (a) capillary force vaporizer, with fuel vapor jetting from central hole, (b) vaporizer unit attached to bottom of burner, with cooling fins and fan, (c) fuel tube, with coiled heater and sidearm connection, and (d) assembled liquid fuel burner, with model airplane piston attached to modulate fuel flow.

Table 1. Composition of JP-8 Surrogate ("Hex-12")

Component	Chemical Class	Molecular Formula	Mole-%	Volume-%
iso-octane	branched alkane	C_8H_{18}	3	3
xylenes	aromatic	C_8H_{10}	15	10
tetralin	cycloalkane/aromatic	$C_{10}H_{12}$	13	9
decalin	cycloalkane	$C_{10}H_{18}$	27	22
dodecane	normal alkane	$C_{12}H_{26}$	30	37
hexadecane	normal alkane	$C_{16}H_{34}$	12	19

For stable operation of the JP-8 surrogate flame, it was found that a small flow of nitrogen through the fuel tube was required to entrain and carry the heavy fuel vapor out of the tube. With JP-8 surrogate vaporized at a rate of 12.5 g/hr (equivalent to 0.0335 slpm), and 0.107 slpm nitrogen supplied to the base of the burner tube, a very stable and repeatable flame was achieved. These flows resulted in 3:1 dilution of the fuel species, reducing the adiabatic flame temperature by approximately 40 K. The resulting smoking flame did not have a well-defined flame height but the strongly luminous zone extended to a height of 40 mm. Figure 3 shows photographs of the three investigated flames and Table 2 provides the flow rates and other information about the flames. The air coflow for both coannular burners was chosen to give optimal stability in the steady flames and was set at 350 slpm, a flow that was considerably higher than that used in the "non-smoking" flame of previous work. In our burners, the flames were found to exhibit strong flickering at these lower airflow rates.

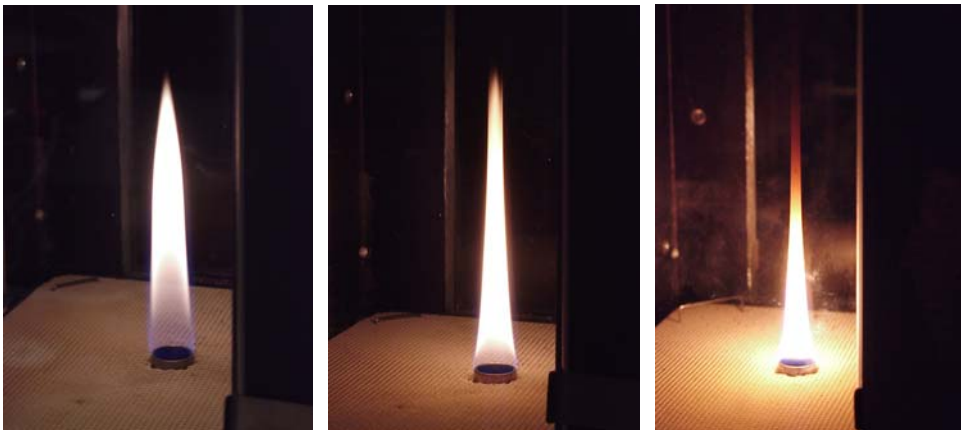

Figure 3: Photographs of steady methane, ethylene, and JP-8 surrogate coannular flames.

Table 2. Characteristics of Investigated Flames

Flame	Q_{fuel} (slpm)	Q_{air} (slpm)	V_{fuel} (cm/s)	V_{air} (cm/s)	tube Re	ϕ [a]	h_f (mm) [b]	T_{ad} (K) [e]
CH_4	0.44	350	8.2	35.3	274	0.012	84	2225
C_2H_4	0.22	350	4.1	35.3	258	0.009	88	2369
JP-8 surrog. + N_2	0.0335 0.107	350	2.6	35.3	41 [c]	0.010	40 [d]	2248

[a] global stoichiometry of gases supplied to the burner
[b] visible flame height
[c] at 327 °C
[d] height of strongly luminous zone (smoking flame without a well-defined flame height)
[e] adiabatic flame temperature, calculated from NASA CEA code

3. Laser and Optical Diagnostics

Several different diagnostic techniques were employed to interrogate these flames, including planar laser-induced fluorescence (PLIF) of OH· and PAH, planar laser-induced incandescence (PLII) measurements of soot concentration, thermopile measurements of local total radiation, and planar graybody emission (from soot). The techniques employed to perform these measurements are described below:

OH· PLIF

A frequency-doubled, Nd:YAG-pumped dye laser provided pulsed ultraviolet light (283 nm) for the planar excitation of OH·, as detailed in Ref. 7. The laser light also excited laser-induced incandescence (LII) emission from the soot particles and broadband fluorescence from polycyclic aromatic hydrocarbons (PAH) [6]. The laser sheet was 50 mm high, with a thickness of 250 μm through the flame zone. The fluorescence and LII signals were collected through a 45-mm focal length, f/1.8 UV Cerco lens attached to a gated, intensified charge-coupled device (ICCD) camera. A Schott WG295 long-pass filter eliminated laser reflections as well as

scattering from soot particles and a 340 nm band-pass filter was used to reduce the signal contribution from soot LII, C_2 Swan band emission, and natural flame emission.

PLII

The fundamental output beam from a Nd:YAG laser provided pulsed infrared light (1064 nm) for excitation of soot LII. This excitation wavelength has been demonstrated to produce negligible interference from PAH fluorescence and does not excite C_2 LIF [24]. A series of lenses and apertures expanded the beam to a laser sheet that was 50 mm high with a small intensity decrease towards the edges of the sheet. To eliminate the influence of this laser intensity falloff, 50-mm high images were collected with a 25 mm overlay. The beam width was 250 μm through the flame zone and the mean laser fluence was 0.5 J/cm^2. The incandescence signal was collected using a UV-grade 450 nm short-pass filter with a 105-mm focal length, f/4.5 UV Nikkor lens attached to an ICCD camera. To minimize irising effects from collecting LII signals on this slow-gating camera, while limiting sensitivity to variations in soot primary particle size and laser fluence, a 400 ns intensifier gate width was used on the ICCD, with the gate opening beginning 100 ns before arrival of the laser pulse. The images were corrected for background and flatfield using the technique described in ref. 25.

The corrected images were calibrated for soot volume fraction by comparing radial soot concentration profiles through mid-heights of the ethylene flame against HeNe laser extinction measurements that had been tomographically inverted using the 3-point Abel technique [26]. The extinction themselves measurements were calibrated for soot volume fraction using the dimensionless extinction coefficient of 9.3 that had been previously determined for the soot in this flame [22]. Note that this value for K_e yields soot concentrations that are roughly a factor of two lower than using Rayleigh-limit absorption coefficients derived from soot index of refraction values in the literature (as is commonly done in the combustion literature). However, there is a strong body of evidence supporting K_e values between 8 and 10 [22,27].

Thermopile Measurements

The local radiant heat flux from the flames was measured using a thin-film thermopile with a CaF_2 window and a 150 mm long sight tube with an ID of 2 mm. The sight tube was anodized to minimize light reflections. The use of the CaF_2 window material makes the radiometer equally sensitive to radiant emission from 0.13–11 μm, encompassing nearly all of the energy-containing radiation from the flame. The thermopile that was chosen for this measurement is 2 mm x 2 mm in size. The radiometer was calibrated by mounting it in front of a high-temperature blackbody source, whose display temperature was verified with a type-R fine-wire thermocouple. The temperature of the thermopile was closely monitored during measurements and calibrations because of the sensitivity of the thermopile response to temperature.

Soot Graybody Emission

Images of soot graybody emission were captured by two ICCD cameras, at right angles to one another, that imaged the flame through a large beamsplitter. Narrow bandpass filters at 700 nm and 850 nm were used to image the soot layer at specific wavelengths free from significant gas-band radiation.

4. Results and Discussion

Figure 4 shows OH· PLIF images of the methane, ethylene, and JP-8 surrogate flames. The higher soot concentrations in the ethylene and JP-8 surrogate flames are evident in the strong LII signals that compete with the OH· signals. The JP-8 surrogate flame also shows very strong broadband fluorescence (usually associated with PAH) at the bottom of the flame, where the fuel stream exits the fuel tube. The collapse of the OH· layer along the side of the JP-8 surrogate flame is also evident, consistent with the observation that this is a strongly smoking flame.

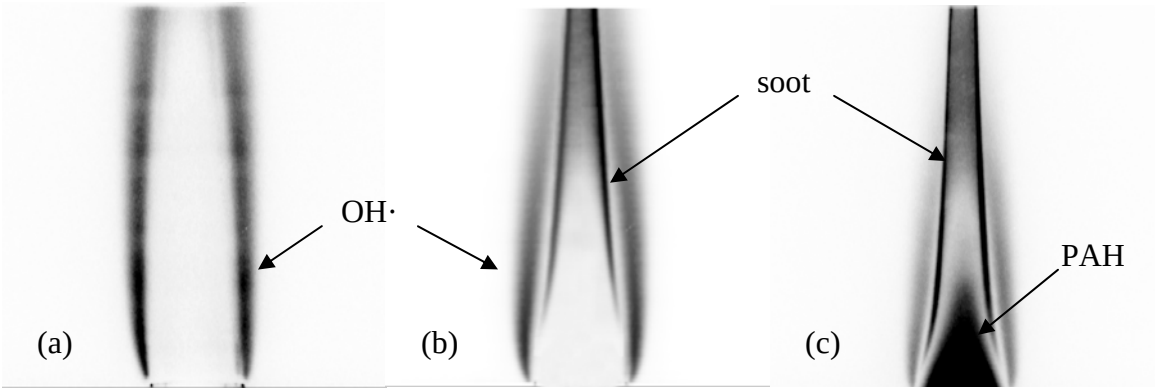

Figure 4: OH· PLIF of the bottom 50 mm of the (a) methane, (b) ethylene, and (c) JP-8 surrogate flames.

Figure 5 shows the calibrated LII images for the methane, ethylene, and JP-8 surrogate flames. Despite the nitrogen dilution of the JP-8 surrogate, which reduces soot formation through fuel species dilution and lower flame temperatures [28,29], the JP-8 flame produces higher soot concentrations than ethylene and shows significant soot concentrations earlier in the flame (helping to contribute, through radiative losses, to the quenching of the OH· layer). The overall migration of the sooting region from the interior areas for low sooting flames (methane) to the annular region for strongly sooting flames (JP-8) is readily apparent in Fig. 5.

Figure 6 shows the total radiative emission measured at selected heights of the flames using the calibrated thermopile. As expected, the methane flame shows lower radiation than the more heavily sooting ethylene and JP-8 flames. However, the peak emission is only 3x higher for the ethylene and JP-8 flames, showing the non-negligible contribution of gas-band emission to the total radiation (particularly for the methane flame). The similarity in the magnitude of the local radiative emission from the ethylene and JP-8 flames is interesting, though the earlier formation of soot for JP-8 is clearly evident in the rapid rise in the radiative flux. The JP-8 flame also reaches its peak emission at the approximate location at which the OH· layer is collapsing (and the soot layer begins to cool) whereas the ethylene flame has its peak emission at mid-flame height, where the soot begins to undergo significant oxidization.

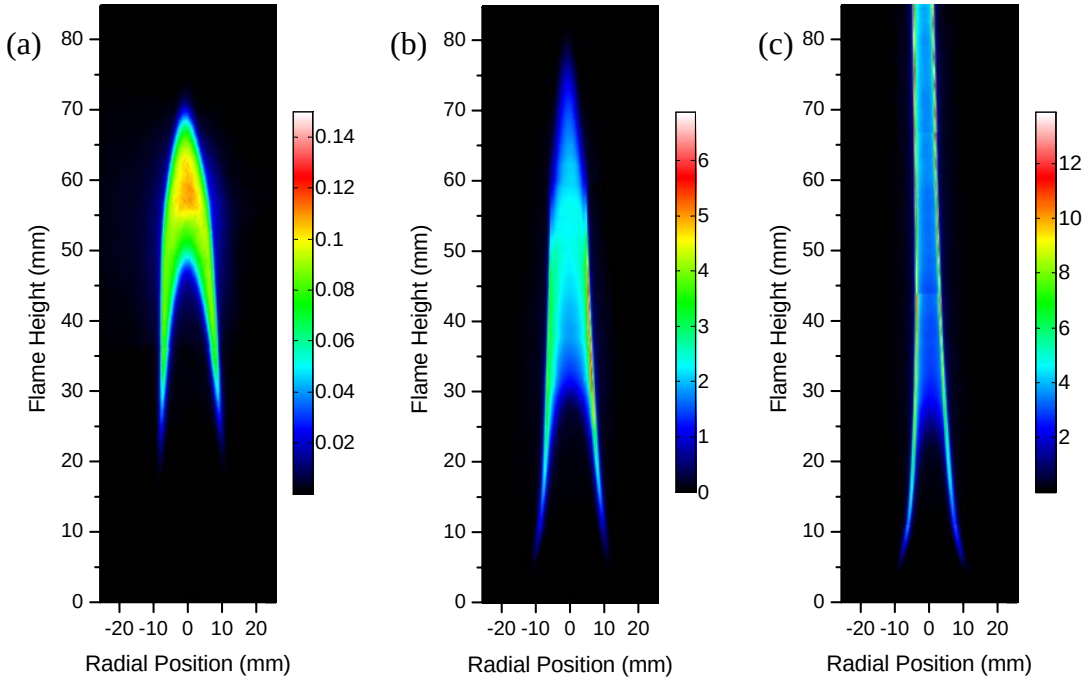

Figure 5: Calibrated, stacked LII images of soot concentrations in the (a) methane, (b) ethylene, and (c) JP-8 surrogate flames. The color legends on the sides of the figures indicate the soot concentration, in ppm.

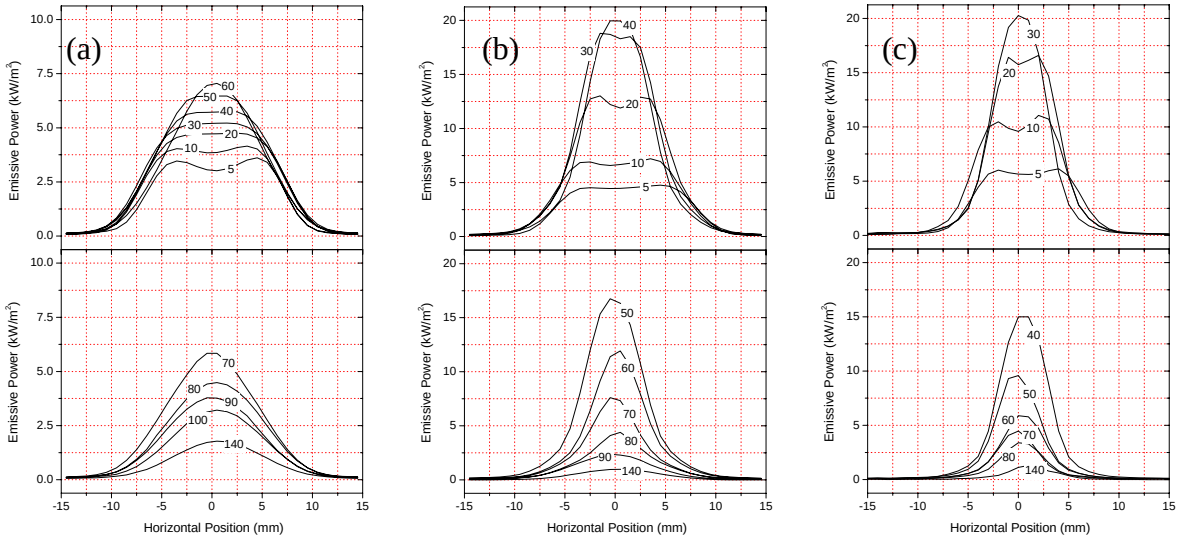

Figure 6: Radial profiles of the local radiative emission from the (a) methane, (b) ethylene, and (c) JP-8 surrogate flames. The top figures give the data for the lower flame heights and the bottom figures give the data for the upper flame heights. Note the 2x lower scaling of the ordinate for the methane flame.

5. Concluding Remarks

Several laser and optical diagnostic techniques have been employed in the interrogation of laminar jet diffusion flames burning methane, ethylene, and a JP-8 surrogate fuel, diluted by nitrogen. The experimental measurements allow comparisons to be made in the overall flame structure, soot formation tendency, and thermal radiation fields from these different flames. Despite 3:1 dilution by nitrogen, the JP-8 surrogate forms soot earlier than ethylene and shows peak soot concentrations that are twice those of ethylene. The local thermal radiation from the JP-8 surrogate flame is approximately equal to that of the ethylene flame, while the methane flame has ~ 3x lower radiant intensity.

Acknowledgments

This work was supported by a Laboratory Directed Research and Development project at Sandia National Labs. Bob Harmon and Matt Boisselle of Sandia assisted in laboratory measurements. Sandia is operated by the Sandia Corporation, a Lockheed Martin Company, for the U.S. DOE under contract DE-AC04-94-AL85000.

References

[1] K.C. Smyth, J.E. Harrington, E.L. Johnsson, W.M. Pitts, *Combust. Flame* 95 (1993) 229-239.
[2] C.R. Shaddix, J.E. Harrington, K.C. Smyth, *Combust. Flame* 99 (1994) 723-732.
[3] C.R. Shaddix, K.C. Smyth, *Combust. Flame* 107 (1996) 418-452.
[4] D.A. Everest, C.R. Shaddix, K.C. Smyth, *Proc. Combust. Inst.* 26 (1996) 1161-1169.
[5] R.R. Skaggs, J.H. Miller, *Proc. Combust. Inst.* 26 (1996) 1181-1188.
[6] K.C. Smyth, C.R. Shaddix, D.A. Everest, *Combust. Flame* 111 (1997) 185-207.
[7] C.R. Shaddix, T.C. Williams, L.G. Blevins, R.W. Schefer, *Proc. Combust. Inst.* 30 (2005) 1501-1508.
[8] T.C. Williams, C.R. Shaddix, R.W. Schefer, P. Desgroux, *Combust. Flame*, in press.
[9] R.J. Santoro, H.G. Semerjian, R.A. Dobbins, *Combust. Flame* 51 (1983) 203-218.
[10] K.C. Smyth, J.H. Miller, R.C. Dorfman, W.G. Mallard, R.J. Santoro, *Combust. Flame* 62 (1985) 157-181.
[11] R.J. Santoro, T.T. Yeh, J.J. Horvath, H.G. Semerjian, *Combust. Sci. Technol.* 53 (1987) 89-115.
[12] R. Puri, T.F. Richardson, R.J. Santoro, R.A. Dobbins, *Combust. Flame* 92 (1993) 320-333.
[13] I.M. Kennedy, C. Yam, D.C. Rapp, R.J. Santoro, *Combust. Flame* 107 (1996) 368-382.
[14] I. Glassman, *Proc. Combust. Inst.* 22 (1988) 295-311.
[15] T. Edwards, L.Q. Maurice, *J. Prop. Power* 17 (2001) 461-466.
[16] A. Violi, S. Yan, E.G. Eddings, A.F. Sarofim, S. Granata, T. Faravelli, E. Ranzi, *Combust. Sci. Technol.* 1747(2002) 399-417.
[17] A. Agosta, N.P. Cernansky, D.L. Miller, T. Faravelli, E. Ranzi, *Expt. Thermal Fluid Sci.* 28 (2004) 701-708.
[18] E.G. Eddings, S. Yan, W. Ciro, A.F. Sarofim, *Combust. Sci. Technol.* 177 (2005) 715-739.
[19] I.M. Aksit, J.B. Moss, *Fuel* 84 (2005) 239-245.
[20] J.B. Moss, I.M. Aksit, *Proc. Combust. Inst.* 31 (2007) 3139-3146.
[21] J.A. Cooke, M. Bellucci, M.D. Smooke, A. Gomez, A. Violi, T. Faravelli, E. Ranzi, *Proc. Combust. Inst.* 30 (2005) 439-446.
[22] T.C. Williams, C.R. Shaddix, K.A. Jensen, J.M. Suo-Anttila, *Int. J. Heat Mass Trans.* 50 (2007) 1616-1630.
[23] C.M. Megaridis, R.A. Dobbins, *Combust. Sci. Technol.* 66 (1989) 1-16.
[24] R.J. Santoro, C.R. Shaddix, in: K. Kohse-Hoinghaus, J.B. Jeffries (Eds.), Applied Combustion Diagnostics, Taylor & Francis, New York, 2002, Ch. 9, pp. 252-286.
[25] T.C. Williams, C.R. Shaddix, submitted to *Rev. Sci. Instruments.*
[26] C.J. Dasch, *Appl. Optics* 31 (1992) 1146-1152.
[27] C.R. Shaddix, T.C. Williams, *Amer. Scientist* 95 (2007) 232-239.
[28] I. Glassman, *Proc. Combust. Inst.* 27 (1998) 1589-1596.
[29] H. Guo, F. Liu, G.J. Smallwood, O.L. Gulder, *Proc. Combust. Inst.* 29 (2002) 2359-2365.